

RETRIEVAL OF AEROSOL OPTICAL DEPTH FROM MODIS DATA
AT 500 M RESOLUTION COMPARED WITH GROUND
MEASUREMENT IN THE STATE OF INDIANA

Fahed Alhaj Mohamad

Submitted to the faculty of the University Graduate School

in partial fulfillment of the requirements

for the degree

Master of Science

in the Department of Geography,

Indiana University

May 2015

Accepted by the Graduate Faculty, Indiana University, in partial fulfillment of the requirements for the degree of Master of Science.

Master's Thesis Committee

Daniel P. Johnson, Ph.D., Chair

Vijay O. Lulla, Ph.D.

Frederick L. Bein, Ph.D.

ACKNOWLEDGMENTS

I would like to express my gratitude to my supervisor Professor Daniel Johnson for his supervision, remarks and contribution to this study. Prof Dan has given me great deals of valued and precious ideas and useful comments throughout my learning process of this master thesis, and has been a tremendous mentor for me.

I am gratefully thankful to the research committee Professor Frederick Bein and Vijay Lulla for their advices, comments and administration. I would also sincerely thank the staff and colleagues in the Department of Geography at IUPUI. Especially Aaron Pierce, Peng Jin, April Douglas, Jeff Ashby and Joyce Haibe.

Special thanks to the Fulbright Program and my advisors at AMIDEAST who supported me throughout my journey, John Orak, Anna Palaguta, Emmanuel Pimentel, and Mathew Guckenberger.

Words cannot express how grateful I am to my family for all of the sacrifices that they have made on my behalf. Your prayer for me was what sustained me thus far. I would also like to thank all of my friends who supported me in writing, and incited me to strive towards my goal.

I would like to dedicate this work in honor and memory of my deceased mother who taught me invaluable lessons in life, may her soul rest in peace. Also to the great man in my life, my father!

TABLE OF CONTENTS

LIST OF TABLES v

LIST OF FIGURES vi

LIST OF ABBREVIATIONS vii

INTRODUCTION 1

 Background and Significance 2

 Applications for Aerosol Optical Depth 5

 Remote Sensing Approaches 5

 Objectives 7

LITERATURE REVIEW 8

STUDY AREA 10

DATA USED 11

 The Aerosol Robotic Network (AERONET) 11

 PM_{2.5} Ground Measurements 12

 MODerate Resolution Imaging Spectroradiometer (MODIS) 14

METHODOLOGY 21

RESULTS 23

DISCUSSION 28

APPENDICES 30

BIBLIOGRAPHY 37

CURRICULUM VITAE

LIST OF TABLES

| | |
|---|----|
| Table 1: MODIS spectral bands and their primary usage | 15 |
| Table 2: Summary of Level 1B Products: | 18 |
| Table 3: Regression analysis of the AOD and PM values for August 1 st 2012 | 25 |

LIST OF FIGURES

| | |
|---|----|
| Figure 1: Size distribution of different types of airborne particles | 2 |
| Figure 2: Polutants pumbed into the air from Harding Street plant | 3 |
| Figure 3: Aerosol product from MOD04_L2 for August 1st 2012 | 6 |
| Figure 4: Location of Indiana State | 10 |
| Figure 5: AERONET locations around the study area of Indiana State | 11 |
| Figure 6: PM _{2.5} monitoring network in Indiana State..... | 13 |
| Figure 7: False color image at 500m Resolution of Indiana State on August 1, 2012. MODIS bands 6, 2 and 7 were used to construct the image. | 17 |
| Figure 8: AOD product from August 1st 2012 at 500 m resolution over Mario County..... | 23 |
| Figure 9: MOD04_L2 aerosol product from August 1st 2012 at 10 km resolution over Marion County..... | 23 |
| Figure 10: Surface reflectance product | 23 |
| Figure 11: AOD image from August 1st 2012, with high value of AOD on the edge of the cloud masking.. | 24 |
| Figure 12: AOD from August 1st 2012 using band 4 showing the high values of the AOD over the bright surfaces in Indianapolis. | 25 |
| Figure 13: MOD02HKM product on 10th of August 2012, unusable for analysis | 27 |

LIST OF ABBREVIATIONS

| | |
|---------|--|
| AOD/AOT | Aerosol Optical Depth / Aerosol Optical Thickness |
| EPA | Environmental Protection Agency |
| MODIS | MODerate Resolution Imaging Spectroradiometer Sensor |
| HDF | Hierarchical Data Format |
| PM2.5 | Particulate Matter with a diameter less than 2.5 microns |
| NAAQS | National Ambient Air Quality Standard |
| RTM | Radiative Transfer Model |
| LUT | Look Up Table |
| AERONET | Aerosol Robotic Network |
| MRT | Minimum Reflectance Technique |
| SBDART | Santa Barbara DISORT Atmospheric Radiative Transfer |
| DDV | Dense Dark Vegetation |
| LAADS | Level 1 and Atmosphere Archive and Distribution System |
| MCST | MODIS Characterization and Support Team |
| EV | Earth View |
| NASA | National Aeronautics and Space Administration |
| MAIAC | Multi-Angle Implementation of Atmospheric Correction |
| OBC | On-board calibrator |
| UTM | Universal Transverse Mercator |
| FLAASH | Fast Line-of-sight Atmospheric Analysis of Hypercubes |
| NCDC | National Climatic Data Center |

INTRODUCTION:

According to the National Aeronautics and Space Administration (NASA), Aerosol Optical Depth, τ , tau, also known as aerosol optical thickness, is the degree to which aerosols prevent the transmission of light. The aerosol optical depth or optical thickness (τ) is defined as the integrated extinction coefficient over a vertical column of unit cross section. Extinction coefficient is the fractional depletion of radiance per unit path length (Jo Alfano et al., 2013).

Aerosols are tiny solid and liquid particles suspended in the atmosphere. Examples of aerosols include windblown dust, sea salt, volcanic ash, smoke from fires, and pollution from factories and urban areas. Aerosols have different size distribution, shape and residence time, and derive from different sources: biological contaminants, particulate contaminants, gaseous contaminants, or dust (M. Wong, 2009). Figure 1 is a diagram showing the size distribution in micrometers (μm) of various types of airborne particles.

Based on the size of the aerosols, Environmental Protection Agency (EPA) groups particle pollution into two categories, Particulate matter 10 (PM_{10}) and Particulate matter 2.5 ($\text{PM}_{2.5}$) (EPA_Team, 2013):

- **PM₁₀** "Inhalable coarse particles" such as those found near roadways and dusty industries, are larger than 2.5 micrometers and smaller than 10 micrometers in diameter.
- **PM_{2.5}** "Fine particles," such as those found in smoke and haze, are 2.5 micrometers in diameter and smaller. These particles can be directly emitted from sources such as forest fires, or they can form when gases are emitted from power plants, industries and automobiles react in the air.

The size of particles is directly linked to their potential for causing health problems. EPA is concerned about particles that are 10 micrometers in diameter or smaller because those are the particles that generally pass through the throat and nose and enter the lungs. Once inhaled, these particles can affect the heart and lungs and cause serious health effects (EPA_Team, 2013).

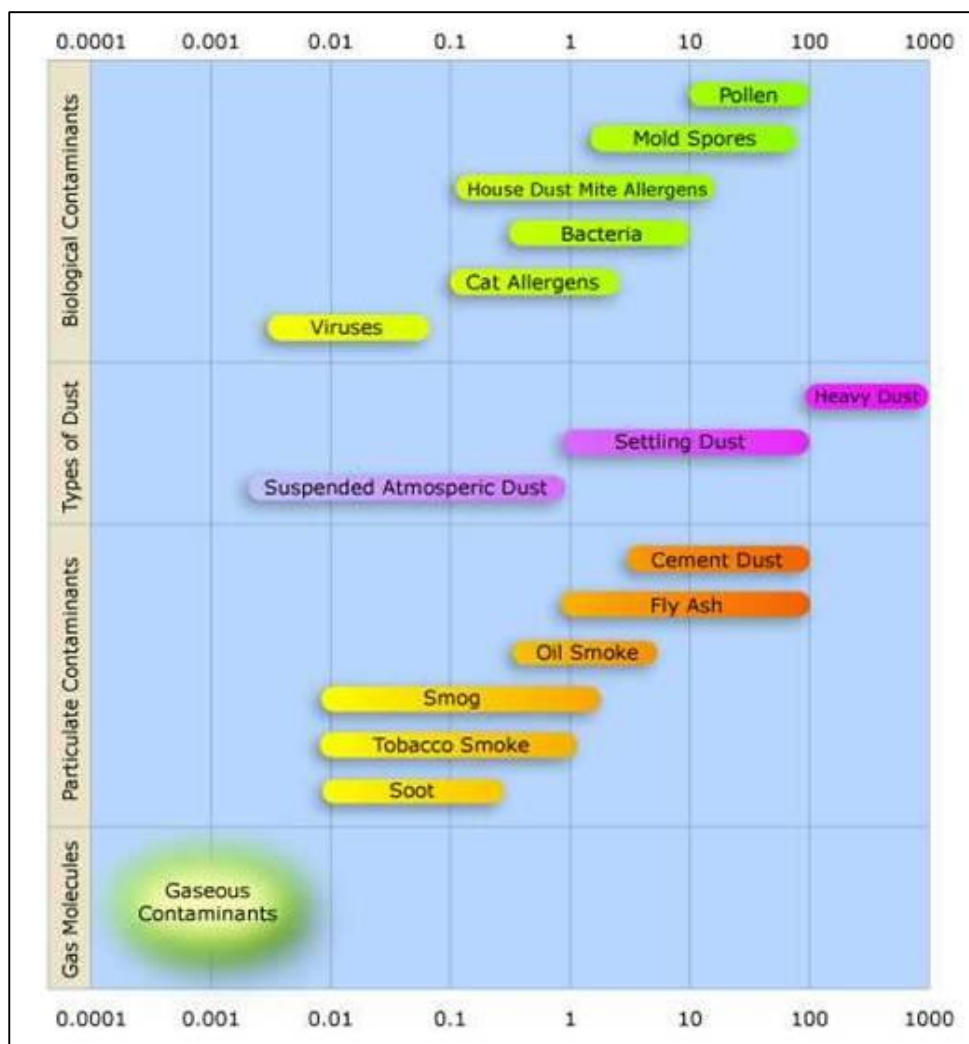


Figure 1: Size distribution of different types of airborne particles in micrometers (μm) (Alam, 2014).

Background and Significance:

Aerosol particles are important to scientists because they represent an area of great uncertainty in their efforts to understand Earth's climate system. Aerosols play an important role in determining the earth's radiation budget and its impact on climate variability by the scattering and absorption of incoming solar energy. They absorb incoming solar radiation which causes a warming effect in the atmosphere, whereas aerosol forcing at the top of the atmosphere may cause a cooling effect by reflecting solar radiation (Bilal, Nichol, Bleiweiss, & Dubois, 2013). Aerosols were known to impact the radiative budget, land surface processes, human health, hydrological processes, and the global carbon, nitrogen and sulfur cycles (Remer, Tanre, Kaufman, Levy, & Mattoo, 2006). Depending upon their

size, type, and location, aerosols can either cool the surface, or warm it. They can help clouds to form, or they can inhibit cloud formation.

Aerosols are of great importance in regards to human health if inhaled, it can be harmful to people's health (Jo Alfano et al., 2013). Based on studies of human populations exposed to high concentrations of particles (sometimes in the presence of SO₂) and laboratory studies of animals and humans, there are major effects of concern for human health. These include effects on breathing and respiratory symptoms, aggravation of existing respiratory and cardiovascular disease, alterations in the body's defense systems against foreign materials, damage to lung tissue, carcinogenesis and premature death. The major subgroups of the population that appear to be most sensitive to the effects of particulate matter include individuals with chronic obstructive pulmonary or cardiovascular disease or influenza, asthmatics, the elderly and children (Seaton, Godden, MacNee, & Donaldson, 1995). Particulate matter also soils and damages materials, and is a major cause of visibility impairment in the United States.



Figure 2: Pollutants pumped into the air from Harding Street plant (Cassell, 2014)

Recent researchers have been focused on fine aerosols for their long-term damage to respiratory system (Dominici, Peng, Bell, & et al., 2006). Numerous epidemiological studies have indicated that exposure to ambient-level fine particulate matter (PM_{2.5}) is

associated with increased morbidity and mortality from cardiovascular and respiratory diseases (Liu et al., 2011).

To even begin to understand the wide-ranging effects of aerosol, it was considered necessary to explain aerosol characteristics with high spatial and temporal resolution (Remer et al., 2006). A full understanding of the impact of aerosol particles in climate and air quality control strategies requires the retrieval of aerosol amounts and characteristics. Spectral aerosol optical depth (AOD) is the relevant satellite-derived parameter most frequently used, because it is the easiest quantitatively useful parameter to obtain (Clarke et al., 2001; Holben et al., 2001, (Bilal et al., 2013). AOD quantifies the extinction of solar radiation at a given wavelength due to presence of aerosols in an atmospheric column (Chudnovsky et al., 2013).

Many remote sensing applications over land require AOD data, e.g. for atmospheric correction. The retrieval of AOD over land is more demanding because the surface reflectance is generally not only higher, so it provides less sensitivity to changes in aerosols, but varies spatially and temporally (Hauser, Oesch, & Wunderle, 2004).

Aerosol Optical Depth (AOD) is a measure of the columnar atmospheric aerosol content (Bilal et al., 2013). It is the measure of aerosols (e.g., urban haze, smoke particles, desert dust, sea salt...) distributed within a column of air from the instrument (Earth's surface) to the top of the atmosphere.

Due to the high temporal resolution of MODIS, the 500 m AOD image can be used to monitor cross-boundary aerosols and the development of pollutant sources (M. Wong, 2009). One of the success stories is the correlations between MODIS aerosol optical depth (AOD) and PM_{2.5} mass concentration which showed that MODIS AOD can be used as an indicator for PM_{2.5} mass concentration, pinpointing the pollution source to local, State, and continental origins, generated by urban/industrial pollution, forest fires, or dust storms (Qu, Gao, Kafatos, Murphy, & Salomonson, 2006). High-resolution AOD is very useful and powerful for urban air quality monitoring and other applications (Y. Li, Xue, He, & Guang, 2012).

Significant body of literature exists shows that ground-level fine particulate matter (PM_{2.5}) can be estimated from columnar AOD. Precision of the measurement of AOD is

$\pm 20\%$ and the prediction of PM_{2.5} from AOD is $\pm 30\%$ in the most careful studies. The air quality needs that can use such predictions are examined (Hoff & Christopher, 2009).

Applications for Aerosol Optical Depth:

There are also many applications for aerosol optical depth (AOD) data:

- 1- Atmospheric correction of remotely sensed surface features.
- 2- Monitoring of sources and sinks of aerosols.
- 3- Monitoring of volcanic eruptions and forest fire.
- 4- Radiative Transfer Model.
- 5- Air Quality.
- 6- Health and Environment.
- 7- Earth Radiation Budget.
- 8- Climate Change (Jo Alfano et al., 2013).

Remote Sensing approaches:

Aerosol detection and monitoring by satellite observations has been substantially developed over past decades, Since 1995, 42 remote sensing instruments relevant to air quality measurements have been put into orbit. Trace gases such as ozone, nitric oxide, nitrogen dioxide, water, oxygen/tetraoxygen, bromine oxide, sulfur dioxide, formaldehyde, glyoxal, chlorine dioxide, chlorine monoxide, and nitrate radical have been measured in the stratosphere and troposphere in column measurements (Hoff & Christopher, 2009).

Satellite data can add synoptic information, visualization, and validation to ground-based air quality data modeling. Satellite data are particularly suited for monitoring the transport of particulate matter since satellite sensors can measure changes in aerosol optical depth over large area (Engel-Cox, Holloman, Coutant, & Hoff, 2004).

The aerosol products available over land from MOD04_L2 product include aerosol optical depth at three visible wavelengths, a measure of the fraction of aerosol optical thickness attributed to the fine mode, and several derived parameters including reflected spectral solar flux at the top of the atmosphere (Remer et al., 2005). However, there remain several major limitations of MOD04_L2 aerosol products for local/urban scale study, including the following:

- (i) It does not retrieve over bright surfaces such as urban and heterogeneous areas.
- (ii) The heterogeneous nature of urban surfaces complicates the derivation of surface reflectances.
- (iii) The 10 km spatial resolution is too coarse to characterize purely local aerosol plumes (M. S. Wong, Nichol, & Lee, 2011).

The **10 km spatial** resolution of the MODIS products only provide meaningful depictions on a broad regional scale like the whole continent or whole world (Figure 3), whereas aerosol monitoring over complex regions such as urban areas, requires more spatial and spectral detail to pinpoint local sources of aerosols.

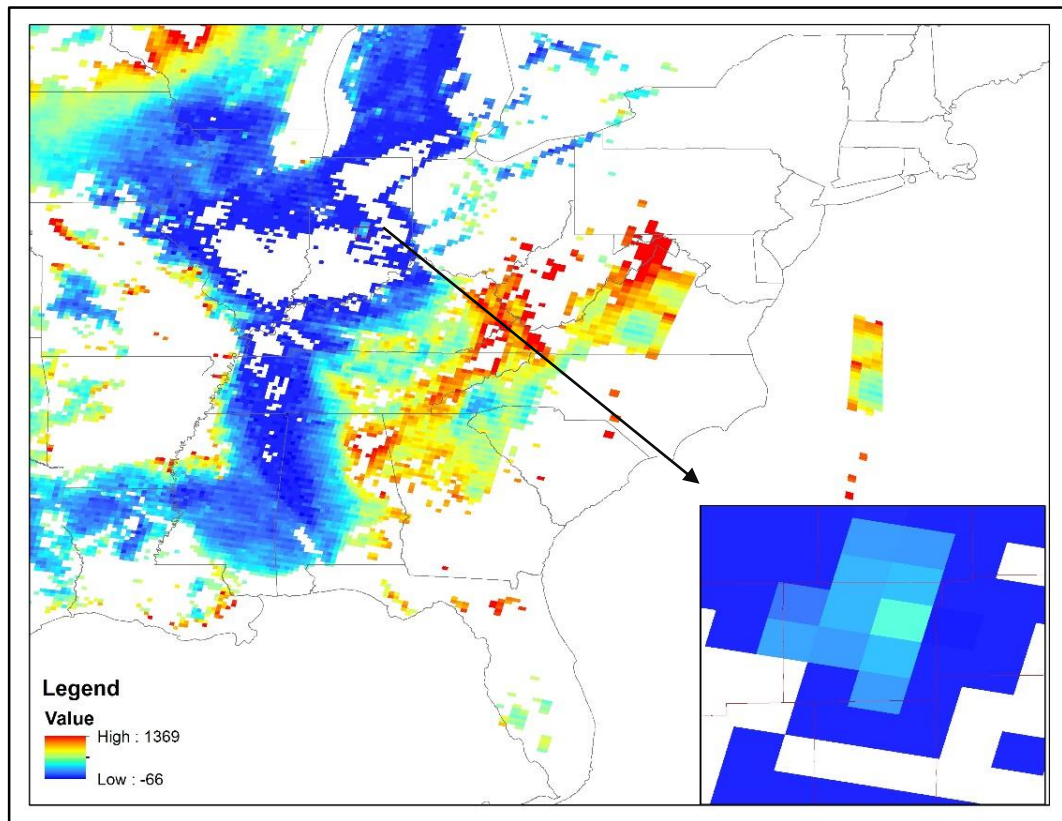


Figure 3: Aerosol product from MOD04_L2 for August 1st 2012.

Objectives:

The purpose of this research is:

- Study the use of Moderate Resolution Imaging Spectroradiometer (MODIS) data in retrieving the aerosol optical depth (AOD) over Indiana State at high resolution of 500 meters.
- Examine the potential of using the resulted AOD data as an indicator of particulate air pollution by comparing the satellite derived AOD data with the ground measurements (provided from the continuous air monitors available over the study area). If an association should be found, AOD data would be used to map particulate matter (PM) concentration.
- Assess current and future ambient concentrations of air pollutants in the State of Indiana using the AOD.

LITERATURE REVIEW:

Following the launch of MODIS, a number of algorithms for aerosol retrieval were developed. Kaufman and Tanré, (1998) first proposed the dense dark vegetation (DDV) method using the multi-wavelength algorithm on the (MODIS) satellite images. The DDV algorithm (called as collection 4) works only on vegetation areas with coverage larger than 60% where the surface reflectances are very low. It prohibits the widespread use of aerosol estimation on the areas of bright surface, such as deserts and urban (Kaufman & Tanré, 1998).

Von Hoyningen-Huene, Freitag, & Burrows, 2003 presented a method based on lookup tables (LUT) between the AOT and the aerosol reflectance for wavelength <0.67 μm . The aerosol reflectance is obtained from TOA reflectance accounting for Rayleigh path reflectance and the apparent spectral surface reflectance (von Hoyningen-Huene, Freitag, & Burrows, 2003).

Hsu et al. (2006) developed a deep blue algorithm for aerosol retrieval over desert, arid, semiarid and urban areas using MODIS images. This algorithm made use of the blue wavelengths where the surface reflectances are bright in red region and darker in blue region. In order to infer the aerosol information, a surface reflectance database was developed based on the minimum reflectance technique (MRT) (Koelemeijer, De Haan, & Stammes, 2003). The accuracy of resulting AOT was validated with a good agreement (within 30%) with AERONET ground measurements (Hsu, Tsay, King, & Herman, 2006).

Li et al. (2005) developed a 1 km AOT algorithm based on the MODIS collection 4 algorithm for a study in Hong Kong, but it was limited to dense vegetated areas and validated using handheld sunphotometers over non-urban surfaces only (C. Li, Lau, Mao, & Chu, 2005).

Lee et al. used similar technique on the estimation of the surface reflectance for the aerosol retrieval in Korea (Kwon Ho, Young Joon, von Hoyningen-Huene, & Burrow, 2006). This technique indicates the advantageous on aerosol observation over bright surface areas.

Wong, (2009) developed a new aerosol retrieval algorithm for the MODIS 500m resolution data to retrieve aerosol properties over land, which helps on addressing the aerosol climatic issues in local/urban scale. The rationale of his proposed aerosol retrieval

algorithm is to determine the aerosol reflectance by decomposing the top-of-atmosphere (TOA) reflectance from surface reflectance and the Rayleigh path reflectance (M. Wong, 2009).

Li et al., (2012) presented a new aerosol retrieval algorithm that applies the synergetic use of small satellite data and MODIS data. The algorithm was applied to data from the China HJ-1A/1B of the Environment and Disasters Monitoring Microsatellite Constellation Charge-Coupled Device (CCD) camera and Terra MODIS data. To downscale 500 m MODIS data, a new method based on mutual information was developed. By applying this algorithm to aerosol retrieval over Beijing City, they could obtain the aerosol optical depth (AOD) with a $100\text{ m} \times 100\text{ m}$ resolution (Y. Li et al., 2012).

Bilal et al., (2013) used MODIS measurements to develop a Simplified Aerosol Retrieval Algorithm (SARA) for use over Hong Kong at high (500 m) spatial resolution, without using a LUT. Instead, RTM calculations were applied directly to the MODIS data, with the aerosol properties derived from a local urban Aerosol Robotic Network (AERONET) station at the Hong Kong Polytechnic University, and surface reflectance from the MOD09GA level-2 daily surface reflectance product (Bilal et al., 2013).

Chudnovsky et al., (2013) developed a new Multi-Angle Implementation of Atmospheric Correction (MAIAC) algorithm for the MODerate Resolution Imaging Spectroradiometer (MODIS), which provides aerosol optical depth (AOD) at 1 km resolution. The relationship between MAIAC AOD and PM_{2.5} as measured by 84 EPA ground monitoring stations in the entire New England and the Harvard super site during 2002–2008 was investigated and also compared to the AOD–PM_{2.5} relationship using conventional MODIS 10 km AOD retrieval from Aqua platform (MYD04) for the same days and locations (Chudnovsky et al., 2013).

STUDY AREA:

Indiana State is located in the Midwestern and Great Lakes regions of North America. With a total area (land and water) of 36,418 square miles (94,320 km²), Indiana ranks as the 38th largest state in size. The state has a maximum dimension north to south of 250 miles (400 km) and a maximum east to west dimension of 145 miles (233 km). The state's geographic center (39° 53.7'N, 86° 16.0'W) is in Marion County. The highest point is the Hoosier Hill (383m) and the lowest point at Ohio River (98m), while the average elevation of Indiana is about 700 feet (210 m) above sea level. Indiana has a humid continental climate, with cold winters and warm, wet summers (wikipedia, Retrieved November 1st 2014).

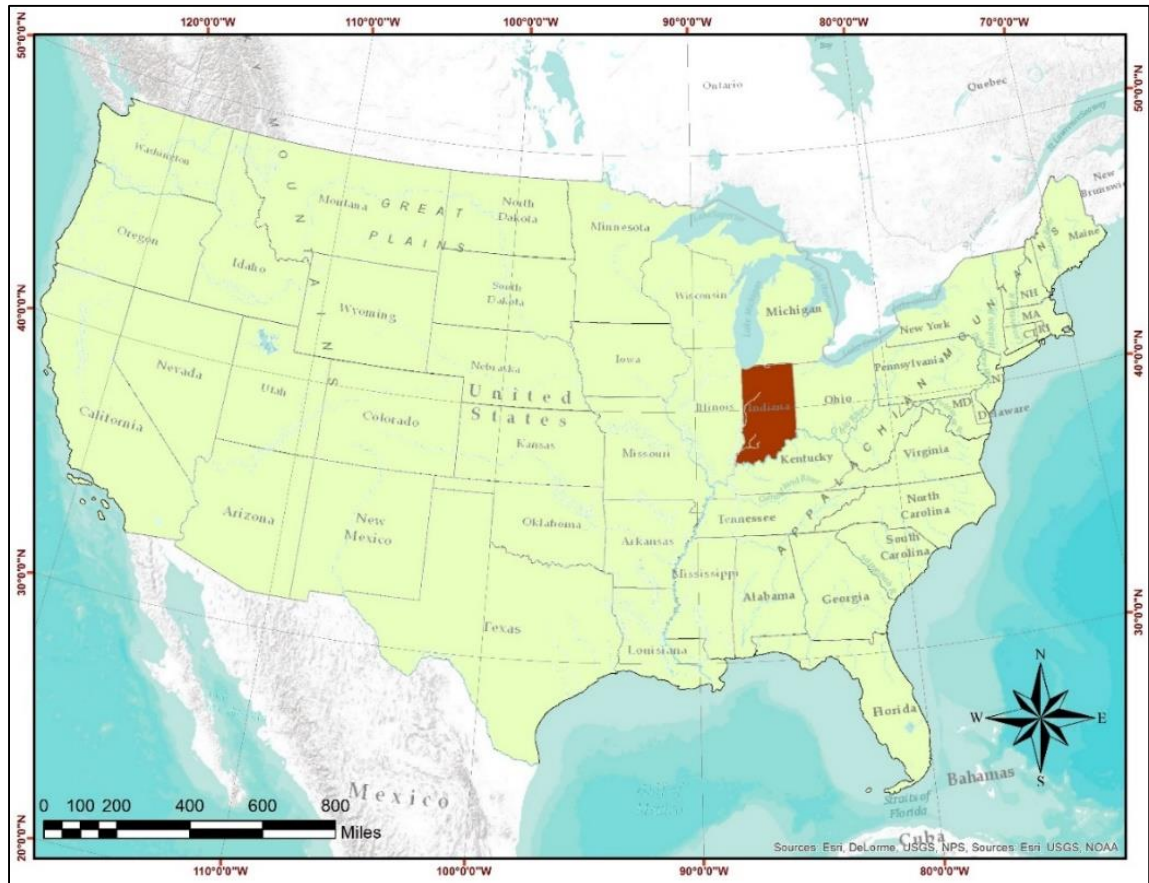


Figure 4: Location of Indiana State

DATA USED:

The Aerosol Robotic Network (AERONET):

Measurements of aerosols have progressed significantly since the establishment of ground-based monitoring networks, such as the AEROSOL ROBOTIC NETWORK (AERONET). Most of the literature on extracting AOD have used data from AERONET to correlate it with their AOD derived from MODIS in order to validate their results.

AERONET is a global, collaborative network that accurately measures spectral aerosol optical depth, and derives many useful, radiatively-equivalent, column-average, aerosol properties from sun/sky radiance measurements. It consists of sunphotometers for measuring the aerosol extinction every fifteen minutes using multiple wavelengths radiometer (M. Wong, 2009).

Unfortunately, in this study there is no AERONET data over Indiana State to validate the resulted AOD, instead ground measurement of PM_{2.5} will be used to predict the validity of the derived AOD, Figure 5.



Figure 5: AERONET locations in the Midwest region of United States.

Ground measurements of PM_{2.5}:

Air quality monitoring has long relied on ground measurement at point monitoring sites. Annual and 24-hour National Ambient Air Quality Standards (NAAQS) for particulate matter were first set in 1971. The federal Clean Air Act, which was passed in 1970 and last amended in 1990, requires United States Environmental Protection Agency (U.S. EPA) to set National Ambient Air Quality Standards (NAAQS) for pollutants that cause adverse effects to public health and the environment. Due to this, ground monitors are placed strategically across the nation to provide air samples that are tested for information about what is contained in the air. PM_{2.5} data is collected across Indiana by the Indiana Department of Environmental Management's (IDEM) Office of Air Quality. IDEM operates 14 continuous PM_{2.5} monitoring sites that are polled hourly in order to obtain the most current information (IDEM PM_{2.5} data map, 2014). Figure 6, shows the locations of the PM_{2.5} monitoring sites in Indiana.

Routine measurements of ground-level PM_{2.5} concentrations using air quality monitoring networks are of great importance in assessing exposures, but ground monitoring data often lacks spatially and temporally complete coverage.

In recently years, repetitive and broad coverage capabilities of satellites allow atmospheric remote sensing to offer a unique opportunity to monitor air quality at continental, national and regional scales. Aerosol optical depth (AOD) data from MODIS could be used to improve ground measurement of fine particulate matter (Hu, 2009).

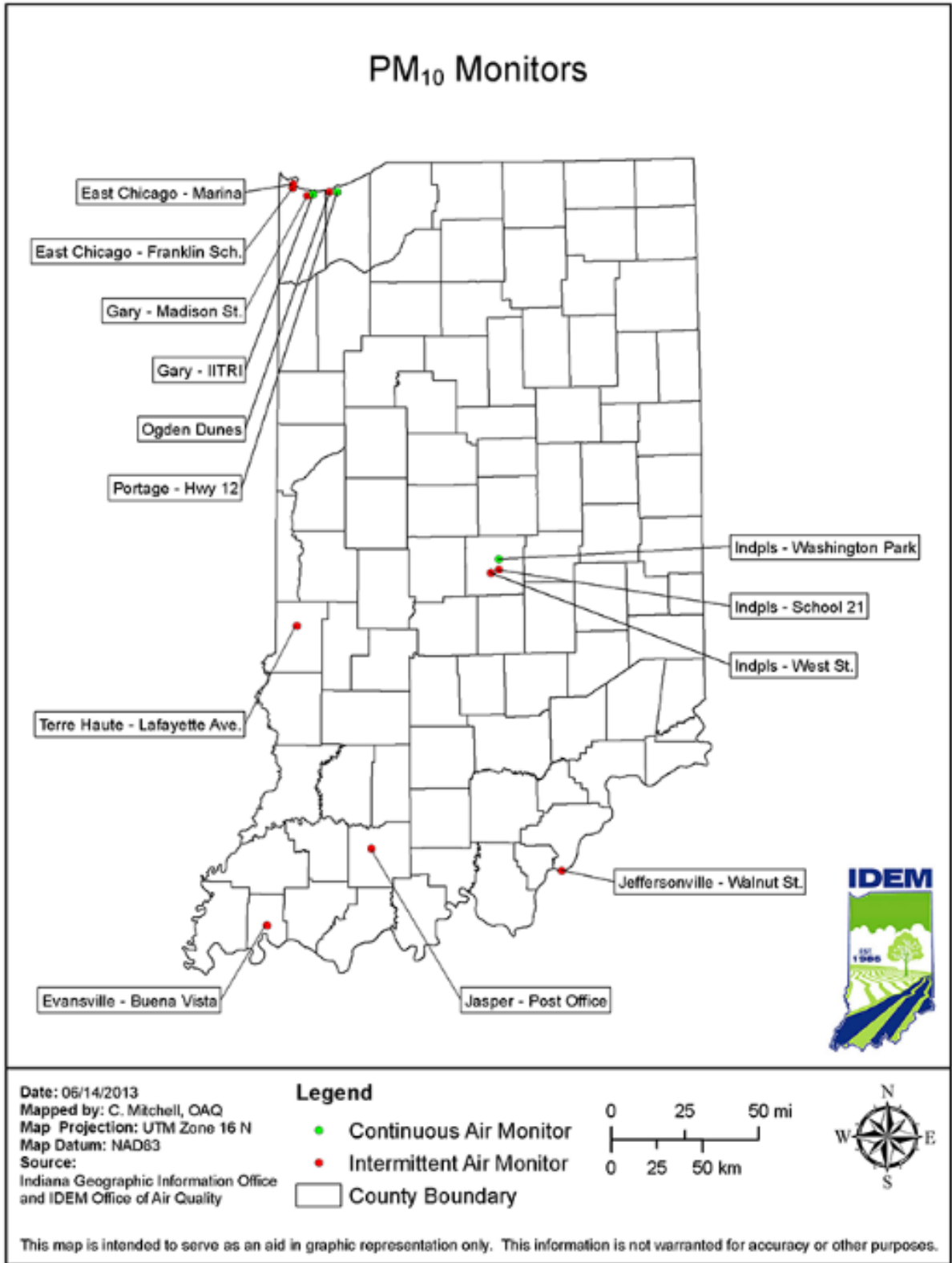


Figure 6: PM_{2.5} monitoring network in Indiana State (IDEM)

MODerate Resolution Imaging Spectroradiometer (MODIS):

Measurements of ground-level PM_{2.5} concentrations by air quality monitoring networks are of great importance in assessing exposures, but their spatial coverage is limited. In addition, the coarse spatial resolution of the MODIS AOD products (10 km) only provide meaningful depictions on a broad regional scale and suitable for global research, whereas aerosol monitoring over Indiana requires more spatial and spectral detail. For this reason the satellite remote sensing can be an important tool to complement the ground-level measurements at finer spatial resolutions (Chudnovsky et al., 2013).

A large number of satellite data products for multiple disciplines of land and atmosphere studies can be generated from the raw remote sensing data. For example, the data from the MODIS sensor can generate 14 different products. Each data product may contain up to 50 different variables. These data products, derived from the satellite observations, describe features of the land, oceans and atmosphere and are used to study processes and changing trends in real-time environmental remote sensing research and applications for both the local and global scales (Zhao, Wu, Veeramacheneni, Song, & Biehl, 2009).

Prior to MODIS, satellite measurements were limited to reflectance measurements in one (GOES, METEOSAT) or two (AVHRR) channels. There was no real attempt to retrieve aerosol content over land on a global scale. Algorithms had been developed for use only over dark vegetation. The blue channel on MODIS, not present on AVHRR, offers the possibility to extend the derivation of optical thickness over land to additional surfaces (Remer et al., 2006).

MODIS has the ability to characterize the spatial and temporal characteristics of the global aerosol field. Launched aboard NASA's Terra and Aqua satellites in December 1999 and May 2002, MODIS has 36 channels spanning the spectral range from 0.41 to 15 μm representing three spatial resolutions: 250 m (2 channels), 500 m (5 channels), and 1 km (29 channels). The aerosol retrieval makes use of seven of these channels (0.47–2.13 μm) to retrieve aerosol characteristics and uses additional wavelengths in other parts of the spectrum to identify clouds and river sediments (Ackerman et al. 1998; Gao et al. 2002; Martins et al. 2002; Li et al. 2003 (Remer et al., 2005).

The algorithms for retrieving aerosols take advantage of the MODIS wide spectral range and high spatial resolution with daily global coverage (e.g., 500 m at 0.47 to 2.13 μm with 250 m at 0.66 and 0.86 μm and 1 km at 3.8 μm) (Kaufman & Tanré, 1998).

Table 1: MODIS spectral bands and their primary usage (NASA, Retrieved November 7th, 2014):

| Primary Use | Band | Bandwidth ¹ | Spectral Radiance ² | Required SNR ³ |
|---|------|------------------------|--------------------------------|-------------------------------------|
| Land/Cloud/Aerosols Boundaries | 1 | 620 - 670 | 21.8 | 128 |
| | 2 | 841 - 876 | 24.7 | 201 |
| Land/Cloud/Aerosols Properties | 3 | 459 - 479 | 35.3 | 243 |
| | 4 | 545 - 565 | 29.0 | 228 |
| | 5 | 1230 - 1250 | 5.4 | 74 |
| | 6 | 1628 - 1652 | 7.3 | 275 |
| | 7 | 2105 - 2155 | 1.0 | 110 |
| Ocean Color/ Phytoplankton/ Biogeochemistry | 8 | 405 - 420 | 44.9 | 880 |
| | 9 | 438 - 448 | 41.9 | 838 |
| | 10 | 483 - 493 | 32.1 | 802 |
| | 11 | 526 - 536 | 27.9 | 754 |
| | 12 | 546 - 556 | 21.0 | 750 |
| | 13 | 662 - 672 | 9.5 | 910 |
| | 14 | 673 - 683 | 8.7 | 1087 |
| | 15 | 743 - 753 | 10.2 | 586 |
| | 16 | 862 - 877 | 6.2 | 516 |
| Atmospheric Water Vapor | 17 | 890 - 920 | 10.0 | 167 |
| | 18 | 931 - 941 | 3.6 | 57 |
| | 19 | 915 - 965 | 15.0 | 250 |
| <hr/> | | | | |
| Primary Use | Band | Bandwidth ¹ | Spectral Radiance ² | Required NE[delta]T(K) ⁴ |
| Surface/Cloud Temperature | 20 | 3.660 - 3.840 | 0.45(300K) | 0.05 |
| | 21 | 3.929 - 3.989 | 2.38(335K) | 2.00 |
| | 22 | 3.929 - 3.989 | 0.67(300K) | 0.07 |
| | 23 | 4.020 - 4.080 | 0.79(300K) | 0.07 |

| | | | | |
|--|----|-----------------|------------|----------|
| Atmospheric Temperature | 24 | 4.433 - 4.498 | 0.17(250K) | 0.25 |
| | 25 | 4.482 - 4.549 | 0.59(275K) | 0.25 |
| Cirrus Clouds Water Vapor | 26 | 1.360 - 1.390 | 6.00 | 150(SNR) |
| | 27 | 6.535 - 6.895 | 1.16(240K) | 0.25 |
| | 28 | 7.175 - 7.475 | 2.18(250K) | 0.25 |
| Cloud Properties | 29 | 8.400 - 8.700 | 9.58(300K) | 0.05 |
| Ozone | 30 | 9.580 - 9.880 | 3.69(250K) | 0.25 |
| Surface/Cloud Temperature | 31 | 10.780 - 11.280 | 9.55(300K) | 0.05 |
| | 32 | 11.770 - 12.270 | 8.94(300K) | 0.05 |
| Cloud Top Altitude | 33 | 13.185 - 13.485 | 4.52(260K) | 0.25 |
| | 34 | 13.485 - 13.785 | 3.76(250K) | 0.25 |
| | 35 | 13.785 - 14.085 | 3.11(240K) | 0.25 |
| | 36 | 14.085 - 14.385 | 2.08(220K) | 0.35 |
| ¹ Bands 1 to 19 are in nm; Bands 20 to 36 are in μm ² Spectral Radiance values are ($\text{W}/\text{m}^2 \cdot \mu\text{m}\cdot\text{sr}$) ³ SNR = Signal-to-noise ratio ⁴ NE(Δ)T = Noise-equivalent temperature difference | | | | |

For retrieving the AOD at 500 m resolution, the 470, 550, and 660 nm wavebands (bands 3, 4, and 1) of the TERRA/MODIS level 1B calibrated reflectance (MOD02HKM) were collected. In addition, the 10 km resolution MODIS aerosol products (MOD04_L2), surface reflectance product (MOD09), the cloud product (MOD035), and the Geolocation product (MOD03) were collected for comparison purposes.

Level 1B MODIS Data Product Description:

L1B output consists of calibrated earth view (EV) data of all 36 spectral bands, organized in three Hierarchical Data Format (HDF) files corresponding to MODIS' three spatial resolutions, and associated metadata files. These files subsequently serve as the common input for many higher-level science algorithms. A separate file containing on-board

calibrator data sets and key telemetry and geolocation data is also produced by the L1B process (Xiong, Isaacman, & Barnes, 2006).

The purpose of the Level 1B software system, developed by the MODIS Characterization and Support Team (MCST), is to provide calibrated MODIS data for many applications in the area of Earth science. One such application is the construction of images from Level 1B output products (Toller, Isaacman, Leader, & Salomonson, 2003). Figure 7 shows an example of a MODIS image taken from the Level 1B and Atmosphere Archive and Distribution System website (LAADS).

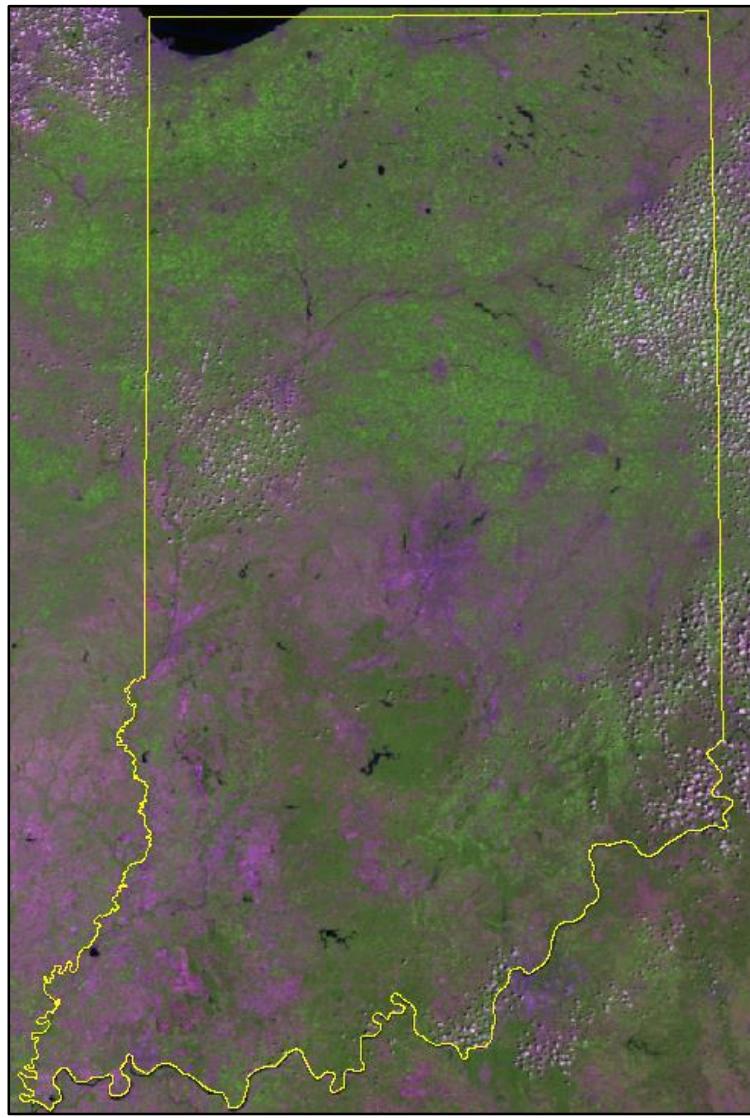


Figure 7: False color image at 500m Resolution of Indiana State on August 1, 2012. MODIS bands 6, 2 and 7 were used to construct the image.

The Level 1B products do not directly contain images such as the one in figure 7; rather they contain the calibrated data used by other software applications to construct the images.

Level 1B software generates three Earth view (EV) product files and one on-board calibrator (OBC) product file (table 2).

Table 2: Summary of Level 1B Products:

| ECS Short Name | | Product Contents |
|-----------------|----------------|--|
| MODIS/ Terra | MODIS/ Aqua | |
| MOD02QKM | MYD02QKM | Calibrated Earth View data at 250m resolution |
| MOD02HKM | MYD02HKM | Calibrated Earth View data at 500m resolution, including the 250m resolution bands aggregated to appear at 500m resolution. |
| MOD021KM | MYD021KM | Calibrated Earth View data at 1km resolution, including the 250m and 500m resolution bands aggregated to appear at 1km resolution. |
| MOD02OBC | MYD02OBC | On Board Calibrator (OBC) and Engineering Data |

- **MODIS Level 1B 250M Earth View Data Product:** contains calibrated Earth View observations for MODIS bands 1 and 2, at 250 meter resolution.
- **MODIS Level 1B 500M Earth View Data Product:** contains calibrated Earth View observations from MODIS bands 3 through 7, at 500-meter resolution. In addition, data from MODIS bands 1 and 2 are each aggregated to appear at the 500 meter resolution.
- **MODIS Level 1B 1KM Earth View Data Product:** contains calibrated Earth View observations from MODIS bands 8 through 36, at 1-kilometer resolution in scientific units. It also contains calibrated data from MODIS bands 1 through 7, each aggregated to appear at the 1km resolution.

The three Earth View (science) products report calibrated data at the three spatial resolutions of 250m, 500m, and 1km. The On Board Calibrator and Engineering Data file contains on-board measurements in the Space View, Black Body, Spectro-Radiometric

Calibration Assembly and Solar Diffuser sectors, and additional engineering data (Toller et al., 2003).

The format of these files is the widely used Hierarchical Data Format (HDF). The architecture of the files utilizes extensions to HDF made with the Hierarchical Data Format- Earth Observing System (HDF-EOS). HDF-EOS is designed to support the data archiving and storage needs of the Earth Observing System (Toller et al., 2003).

HDF is a data model, library, and file format for storing and managing data, developed and maintained by the National Center for Supercomputing Applications at the University of Illinois at Urbana-Champaign. Broadly speaking, HDF is designed to allow sharing of self-describing files across heterogeneous platforms. "Self-describing" means that a data set, such as a multidimensional array of numbers, can have additional metadata logically associated with it that describe things such as the rank of the array, number of elements in each dimension, etc. The ability to access files across heterogeneous platforms is a powerful capability that allows one to read files generated on different machine architecture (Toller et al., 2003).

Level 1B uses the following data objects supported by HDF to store science and calibration data and associated metadata, which describe the scope and quality of science data:

- Scientific data sets (SDS):

These objects contain multidimensional arrays, used to store scientific data. Level 1B employs SDSs to store calibrated science data, their uncertainties, and part of the quality assurance data. The SDSs are made self-describing through a set of attributes — data that may be considered "attached" to the SDS (Toller et al., 2003).

- Fixed length data (vdata):

Level 1B uses vdata to store metadata collected with each rotation of the scan mirror. Vdata may be thought of as a table that consists of a collection of records whose values are stored in fixed-length fields. All records have the same structure and all values in each field have the same data type, in the same way that a database organizes records.

- File (Global) attributes:

HDF attributes can describe the contents of a file as a whole. The Level 1B products use such file or global attributes to record information such as the number of scans and instrument status.

METHODOLOGY:

Aerosol retrieval from satellite remote sensed images aims to retrieve the attenuated radiation by aerosols from the reflection of atmosphere and surface.

In this study, Terra/MODIS 500 m resolution calibrated radiance imagery (MOD02HKM) was acquired from NASA GODDARD Flight Center for retrieval of aerosol over Indiana State. Fast Line-of-sight Atmospheric Analysis of Hypercubes (FLAASH) module in ENVI software was used to georeference MOD02HKM data to UTM zone 16 N coordinate system and North American Datum 1983 (NAD 1983), correct for bow tie effect, radiometric calibration and extraction of top of atmosphere reflectance (TOA).

Rayleigh path reflectance was then calculated based on the computation of spectral dependence of the Rayleigh optical thickness and phase function. This equation is being used for calculating the Rayleigh scattering optical thickness (M. Wong, Nichol, Lee, & Li, 2009) (Bucholtz, 1995):

$$\tau_{Ray}(\lambda) = A \cdot \lambda^{-(B+C\lambda+D/\lambda)} \cdot \frac{P(z)}{P_0}$$

A, B, C, D are the constants of the total Rayleigh scattering cross-section and total Rayleigh volume scattering coefficient at standard atmosphere. The coefficient values of B, C, and D are: 3.55212, 1.35579 and 0.11563 respectively for the wavelengths between 0.2 - 0.5 μm , and 3.99668, 0.00110298 and 0.0271393 for the wavelengths that are greater than 0.5 μm . The coefficient of A takes account of seasonal and latitudinal variations (M. Wong, 2009). For the study area of Indiana State the Midlatitude summer (45° N, July) coefficient value of 0.00651949 for the wavelength between 0.2 - 0.5 μm , and 0.00866735 for the wavelengths that are greater than 0.5 μm were applied.

P(z) is the pressure relevant to the height which is determined by the following parameterized barometric equation:

$$p(z) = P_0 \cdot \exp \left[\frac{-29.87 \cdot g \cdot 0.75 \cdot z}{8.315 \cdot (T_{SURF} - g \cdot 0.75 \cdot z)} \right]$$

The unit of $p(z)$ is Pascal. g is the gravity acceleration (9.807 ms^{-2}), T_{SURF} is the surface temperature in kelvin acquired from the National Climatic Data Center. $p(0)$ is the actual pressure on the sea level (1013 Pa) and z is the height in kilometer. Single value for z over study area was used which is the average height over sea level 0.21 KM.

The next step was to get surface reflectance; which is one of the key products from MODIS and is used in developing several higher-order land products (Vermote, El Saleous, & Justice, 2002).

Getting surface reflectance is an important step in the data processing chain for the extraction of quantitative information in many applications. The estimation of surface reflectance is the key factor in aerosol retrieval, with the aerosol component being the residual (M. S. Wong et al., 2011) (Bilal et al., 2013). MOD09 product from GODDARD Space Flight Center was used for getting the surface reflectance.

Aerosol retrieval then was determined by decomposing the Top-of-Atmosphere (TOA) reflectance derived using FLAASH module in ENVI software from surface reflectance and the Rayleigh path reflectance (Kaufman & Tanré, 1998; M. Wong et al., 2009). The aerosol reflectance then was determined by the following equation:

$$P_{\text{Aer}} = P_{\text{TOA}} - (P_{\text{Surf}} + P_{\text{Ray}})$$

P_{Aer} is aerosol reflectance, P_{TOA} is the top of atmosphere reflectance, P_{Surf} is the surface reflectance and P_{Ray} is the Rayleigh path reflectance.

In order to validate and evaluate the resulted AOD, further analysis has been done to measure the **correlation** between the resulted AOD at band 1 (red) and band 3 (blue) with concentration of the particle matters 2.5 (**PM_{2.5}**) at the surface level which was collected from IDEM.

RESULTS:

The resulted AOD from this study provides much higher details about the local variations of the aerosol distribution compared to the MOD04_L2 aerosol product. Unfortunately, because there is no AERONET measurements available over the study area, calibrating the results using the ground measurements of the AOD by sunphotometers is not possible. PM2.5 monitoring networks cannot be used to validate the AOD from this study, rather just giving a sense of how close the results are to reality. Figure 8 and 9 are a comparison of the AOD from MOD04_L2 at 10 km resolution and AOD from MOD02HKM at 500 m resolution.

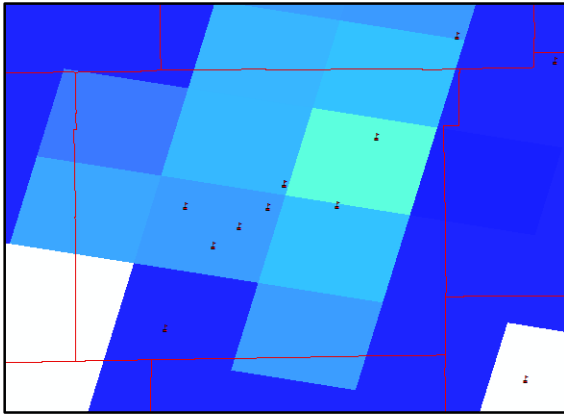


Figure 8: MOD04_L2 aerosol product from August 1st 2012 at 10 km resolution over Marion County

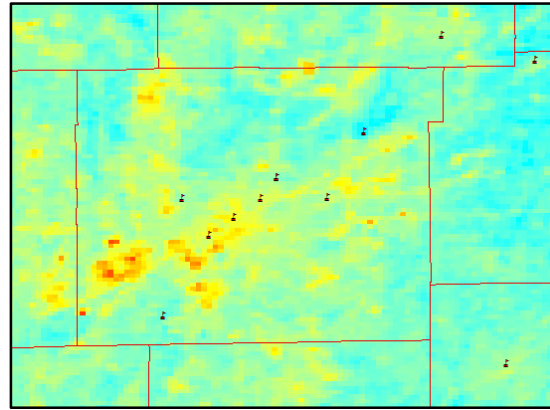


Figure 9: AOD product from August 1st 2012 at 500 m resolution over Marion County

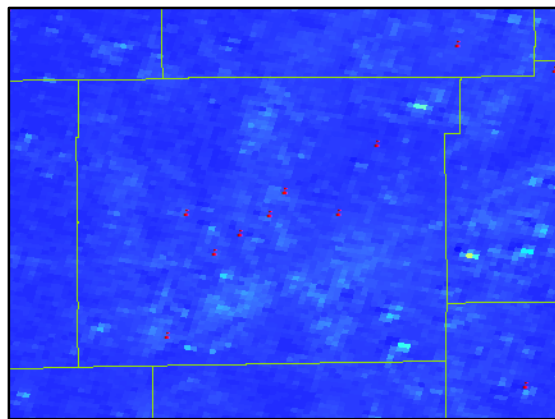


Figure 10: Surface reflectance product

The edges of the cloud masking showing high level of aerosol, because the content of those pixels are mix of cloud and land cover and it is difficult to extract only pure land cover pixels (figure 11).

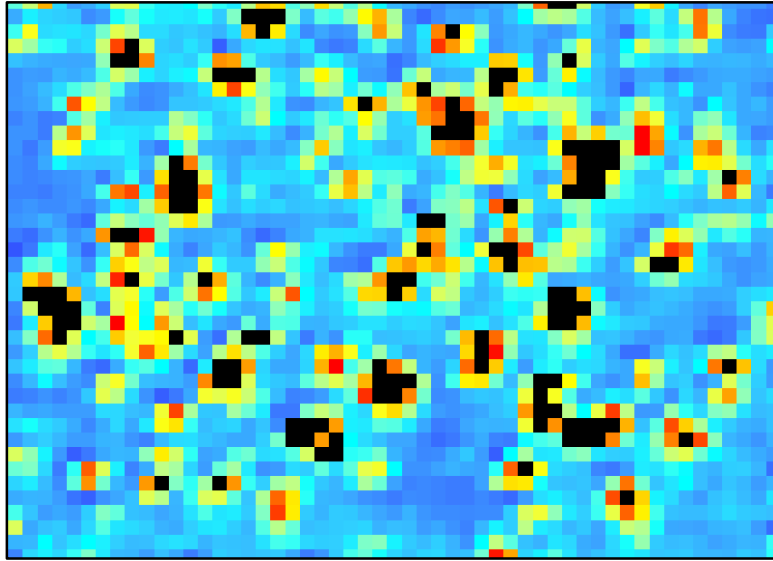


Figure 11: AOD image from August 1st 2012 showing black pixels has no data because of the cloud cover, and high value of AOD on the edge of the masking because of the mixed content.

The bright surfaces in the urban regions are showing high values of AOD (Figure 12), which is causing skewed results, mainly because of the difficulty of differentiating aerosols from bright surfaces. AOD retrieval over urban areas is a difficult task because the measured signal is a composite of reflectance of sunlight by the variable surface covers and back scattering by the semitransparent aerosol layer (Mei et al., 2009). Satellite aerosol remote sensing over urban areas is a more complex task because of the high reflectance of the underlying surface (Y. Li et al., 2012).

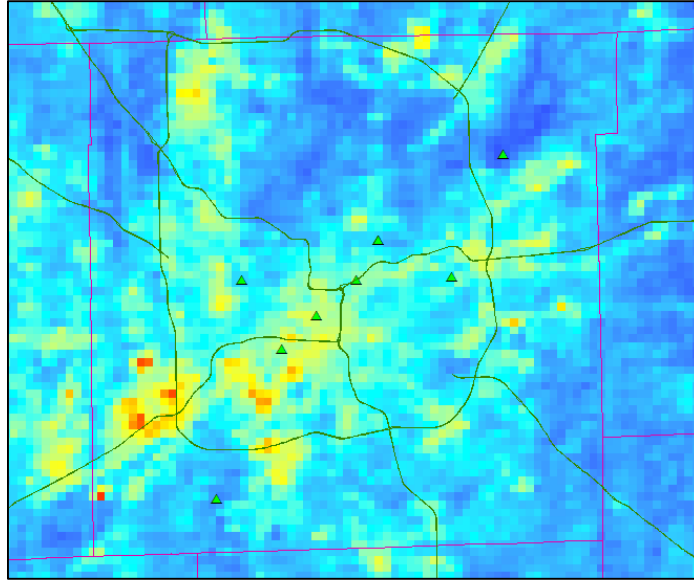


Figure 12: AOD from August 1st 2012 using band 4 showing the high values of the AOD over the bright surfaces in Indianapolis.

The daily measurements of the ground PM_{2.5} monitoring sites and the resulted AOD from band 1 (0.660 μm) and band 4 (0.555 μm) were reasonably correlated. The correlation coefficients (r^2) were between 0.57 and 0.74 (table 3 is an example). In addition, correlation between AOD and PM_{2.5} was higher in suburban areas than in urban areas, this is simply explained by the fact the AOD levels vary very much in the urban areas than in suburban in which it is more homogeneously distributed.

Table 3: Regression analysis of the resulted AOD and PM_{2.5} values for August 1st 2012:

Descriptive Statistics

| | Mean | Std. Deviation | N |
|-----|----------|----------------|----|
| PM | 9.413 | 4.0269 | 15 |
| AOD | .0854380 | .01693539 | 15 |

Correlations

| | | PM | AOD |
|---------------------|-----|-------|-------|
| Pearson Correlation | PM | 1.000 | .675 |
| | AOD | .675 | 1.000 |
| Sig. (1-tailed) | PM | . | .003 |
| | AOD | .003 | . |
| N | PM | 15 | 15 |
| | AOD | 15 | 15 |

Variables Entered/Removed^a

| Model | Variables Entered | Variables Removed | Method |
|-------|-------------------|-------------------|--------|
| 1 | AOD ^b | | Enter |

a. Dependent Variable: PM

b. All requested variables entered.

Model Summary

| Model | R | R Square | Adjusted R Square | Std. Error of the Estimate | Change Statistics | | | | |
|-------|-------------------|----------|-------------------|----------------------------|-------------------|----------|-----|-----|---------------|
| | | | | | R Square Change | F Change | df1 | df2 | Sig. F Change |
| 1 | .675 ^a | .456 | .414 | 3.0827 | .456 | 10.888 | 1 | 13 | .006 |

a. Predictors: (Constant), AOD

ANOVA^a

| Model | | Sum of Squares | df | Mean Square | F | Sig. |
|-------|------------|----------------|----|-------------|--------|-------------------|
| 1 | Regression | 103.475 | 1 | 103.475 | 10.888 | .006 ^b |
| | Residual | 123.542 | 13 | 9.503 | | |
| | Total | 227.017 | 14 | | | |

a. Dependent Variable: PM

b. Predictors: (Constant), AOD

Coefficients^a

| Model | | Unstandardized Coefficients | | Standardized Coefficients | t | Sig. | 95.0% Confidence Interval for B | |
|-------|------------|-----------------------------|------------|---------------------------|--------|------|---------------------------------|-------------|
| | | B | Std. Error | Beta | | | Lower Bound | Upper Bound |
| 1 | (Constant) | -4.302 | 4.232 | | -1.017 | .328 | -13.445 | 4.841 |
| | AOD | 160.531 | 48.649 | .675 | 3.300 | .006 | 55.430 | 265.631 |

a. Dependent Variable: PM

Getting high temporal resolution of the AOD for the local scale regions is also difficult to achieve because of the cloud cover, which makes it hard to retrieve the aerosol optical depth. For the study period from August 1st to August 30th 2012 only six days of MOD02HKM image products were usable for the aerosol retrieval, in the rest of the imagery the cloud cover was higher than 30% over the study area. Figure 13:

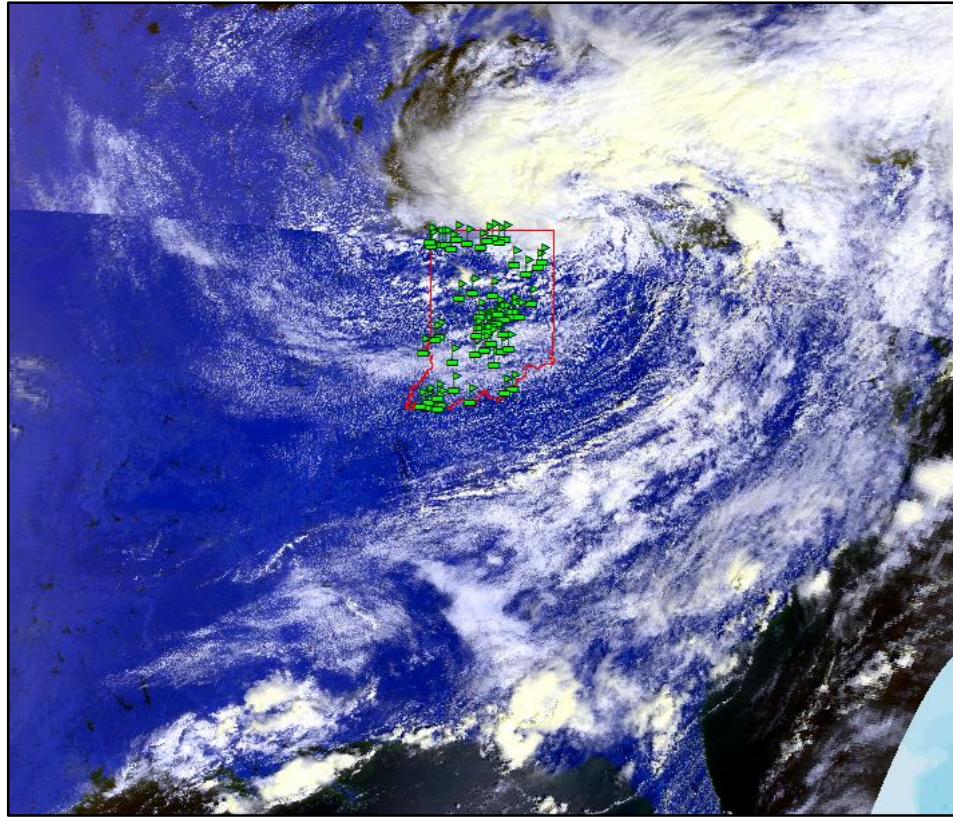


Figure 13: MOD02HKM product on 10th of August 2012, unusable for analysis.

DISCUSSION

Exposure assessments are usually dependent on ground monitoring networks, which lack spatial coverage, especially in rural areas. With rapid technological progress, satellite aerosol remote sensing (AOD) provides a unique opportunity to monitor air quality from space at global, continental, national and regional scales.

There are many factors, which might skew the ground measurements of the PM_{2.5} which in turn would not give an accurate representation on large scale as these measurements are taken close to the ground and values are very varied locally depending on their relative locations to the pollutant sources (highways, factories, coastal areas...etc). Because the satellite-derived AOD is a measure of light attenuation in the column that is affected by ambient conditions (e.g., variable humidity, vertical profile, chemical composition etc.), while PM_{2.5} mass is a measure of dry particles near the surface, these two parameters are not expected to be strictly correlated (Chudnovsky et al., 2013). High AOD values might correspond to low PM surface values, because of the vertical distribution of aerosols.

PM_{2.5} estimation based on satellite AOD on a given day is affected by the choice of which collected EPA PM_{2.5} vs. AOD pair is used due to not only the site location (e.g., proximity to roads) but also due to errors in both PM_{2.5} concentrations and AOD values (Chudnovsky et al., 2013).

Most of the current research on air quality is focusing on developing algorithms for AOD to model ground measurements of the ambient particulate. However, the application of satellite-based exposure assessment in environmental health is still limited, especially for acute effects, because the development of satellite PM_{2.5} model depends on the availability of ground measurements (Liu et al., 2011).

Improving retrievals of aerosol optical depth in a statistical manner normally requires detailed knowledge of uncertainty statistics and bias due to possible error sources such as different measurement viewing geometries, instrument calibration, and dynamically changing atmospheric and earth surface conditions (Albayrak A., 2013).

The possible sources of errors in this study include atmospheric correction, sub-pixel cloud contamination, time gap between MODIS data and measured PM_{2.5}, lack of fixed reference data to calibrate the results, all of these possible sources of error which makes

the retrieval of the AOD a complex process should be taken into full detailed and careful consideration in future research.

Appendix A:

Summary of Science Data Sets in the MODIS Level 1B Earth View Products:

| SDS Name and Description | dim. 1 # bands ¹ | dimension 2 nscans*ndetectors | dimension 3 nframes*namples |
|---|--------------------------------|----------------------------------|--------------------------------|
| 250m product <i>MOD02QKM</i> | | | |
| EV_250_RefSB <i>250m Earth View Science data</i> | 2 | nscans*40 | 1354*4 |
| EV_250_RefSB_Uncert_Indexes <i>Uncertainty Indices for 250m EV reflectance product</i> | 2 | nscans*40 | 1354*4 |
| 500m product <i>MOD02HKM</i> | | | |
| EV_250_Aggr500_RefSB <i>250m Earth View Science data aggregated to 500 m</i> | 2 | nscans*20 | 1354*2 |
| EV_250_Aggr500_RefSB_Uncert_Indexes <i>Uncertainty Indices for 250m EV reflectance product aggregated to 500 m</i> | 2 | nscans*20 | 1354*2 |
| EV_250_Aggr500_RefSB_Samples_Used <i>Number of samples used to aggregate 250m Science data to 500m resolution</i> | 2 | nscans*20 | 1354*2 |
| EV_500_RefSB <i>500m Earth View Science data</i> | 5 | nscans*20 | 1354*2 |
| EV_500_RefSB_Uncert_Indexes <i>Uncertainty Indices for 500m EV reflectance product</i> | 5 | nscans*20 | 1354*2 |
| 1km product <i>MOD021KM</i> | | | |
| EV_250_Aggr1km_RefSB <i>250m EV Science data aggregated to 1 km</i> | 2 | nscans*10 | 1354*1 |
| EV_250_Aggr1km_RefSB <i>Uncertainty Indices for 250m EV reflectance product aggregated to 1 km</i> | 2 | nscans*10 | 1354*1 |
| EV_250_Aggr1km_RefSB_Samples_Used <i>Number of samples used to aggregate 250m Science data to 1km resolution</i> | 2 | nscans*10 | 1354*1 |
| EV_500_Aggr1km_RefSB | 5 | nscans*10 | 1354*1 |

| | | | |
|--|----------------|-----------|--------|
| <i>500m Earth View Science data aggregated to 1 km</i> | | | |
| EV_500_Aggr1km_RefSB_Uncert_Indexes <i>Uncertainty Indices for 500m EV reflectance product aggregated to 1 km</i> | 5 | nscans*10 | 1354*1 |
| EV_500_Aggr1km_RefSB_Samples_Used <i>Number of samples used to aggregate 500m Science data to 1km resolution</i> | 5 | nscans*10 | 1354*1 |
| EV_1KM_RefSB <i>1km EV Science data for Reflective Solar Bands</i> | 15 | nscans*10 | 1354*1 |
| EV_1KM_RefSB_Uncert_Indexes <i>Uncertainty Indices for 1km EV reflectance product</i> | 15 | nscans*10 | 1354*1 |
| EV_1KM_Emissive <i>1km EV Science data for Thermal Emissive Bands</i> | 16 | nscans*10 | 1354*1 |
| EV_1KM_Emissive_Uncert_Indexes <i>Uncertainty Indices for 1km EV thermal emissive radiances</i> | 16 | nscans*10 | 1354*1 |
| EV_Band26 <i>1km EV Science data for band 26</i> | 1 ² | nscans*10 | 1354*1 |
| EV_Band26_Uncert_Indices <i>Uncertainty Indices for Band 26 EV reflectance product</i> | 1 ² | nscans*10 | 1354*1 |

¹ "dim. 1" is the least rapidly varying in each SDS.

² This is implemented as a 2-dimensional SDS because it reports data for only 1 band.

Level 1B MODIS data band grouping and ordering:

| | Number of bands | Bands |
|-----------------------------|------------------------|--|
| The full set of MODIS bands | 38 | 1, 2, 3, 12, 13lo, 13hi, 14lo, 14hi, 15, 16 34, 35, 36 |
| The reflective solar bands | 22 | 1, 2, 3, 12, 13lo, 13hi, 14lo, 14hi, 15, 16, 17, 18, 19, 26 |

| | | |
|--|----|--|
| The thermal emissive bands | 16 | 20, 21, 22, 23, 24, 25, 27, 28, 29, 30, 31, 32, 33, 34, 35, 36 |
| The 250m resolution bands | 2 | 1, 2 |
| The 500m resolution bands | 5 | 3, 4, 5, 6, 7 |
| The 1km resolution reflective bands | 15 | 8, 9, 10, 11, 12, 13lo, 13hi, 14lo, 14hi, 15, 16, 17, 18, 19, 26 |
| The SWIR bands | 4 | 5, 6, 7, 8 |
| Thermal emissive bands which saturate on blackbody warm-up | 3 | 33, 35, 36 |

Summary of the MODIS Level 1B Earth View Product Volume

| Product Name | Day or mixed mode 203-scan granule size (MB) | Night mode 203-scan granule size (MB) | Approximate Daily Volume (GB) | |
|-------------------------------|--|---------------------------------------|---|--|
| | | | Night mode high resolution data production on | Night mode high resolution data production off |
| MOD02QKM | 286.06 | 22.19 | 48.23 | 45.36 |
| MOD02HKM | 275.07 | 22.19 | 46.49 | 43.63 |
| MOD021KM | 343.36 | 142.71 | 72.06 | 54.44 |
| Total Daily Earth View Volume | | | 166.8GB | 143.4GB |

Science Data Sets for MOD09:

| Science Data Sets (HDF Layers (3)) | Units | Data Type | Fill Value | Valid Range | Scale Factor |
|--|-------------|-----------------------|------------|--------------|--------------|
| 250m Surface Reflectance Band 1 (620-670 nm) | Reflectance | 16-bit signed integer | -28672 | -100 - 16000 | 0.0001 |

| | | | | | |
|--|-------------|-------------------------|--------|--------------|--------|
| 250m Surface Reflectance Band 2 (841-876 nm) | Reflectance | 16-bit signed integer | -28672 | -100 - 16000 | 0.0001 |
| 250m Reflectance Band Quality (see Table 14) | Bit Field | 16-bit unsigned integer | 65535 | 0 - 32767 | NA |

Appendix B:

Sizes of airborne particle as dust, pollen bacteria, virus and many more (n.p., Retrieved August 12, 2014):

| Particle | Particle Size (microns) |
|-----------------------|----------------------------|
| one inch | 25400 |
| dot (.) | 615 |
| Eye of a Needle | 1230 |
| Glass Wool | 1000 |
| Spanish Moss Pollen | 150 - 750 |
| Beach Sand | 100 - 10000 |
| Mist | 70 - 350 |
| Fertilizer | 10 - 1000 |
| Pollens | 10 - 1000 |
| Cayenne Pepper | 15 - 1000 |
| Textile Fibers | 10 - 1000 |
| Fiberglass Insulation | 1 - 1000 |
| Grain Dusts | 5 - 1000 |
| Human Hair | 40 - 300 |
| Human Hair | 60 - 600 |
| Dust Mites | 100 - 300 |
| Saw Dust | 30 - 600 |
| Ground Limestone | 10 - 1000 |
| Tea Dust | 8 - 300 |
| Coffee | 5 - 400 |
| Bone Dust | 3 - 300 |
| Hair | 5 - 200 |
| Cement Dust | 3 - 100 |
| Ginger | 25 - 40 |
| Mold Spores | 10 - 30 |

| Particle | Particle Size (microns) |
|--|----------------------------|
| Starches | 3 - 100 |
| Red Blood Cells | 5 - 10 |
| Mold | 3 - 12 |
| Mustard | 6 - 10 |
| Antiperspirant | 6 - 10 |
| Textile Dust | 6 - 20 |
| Gelatin | 5 - 90 |
| Spider web | 2 - 3 |
| Spores | 3 - 40 |
| Combustion-related - motor vehicles, wood burning, open burning, industrial processes | up to 2.5 |
| Fly Ash | 1 - 1000 |
| Milled Flour, Milled Corn | 1 - 100 |
| Coal Dust | 1 - 100 |
| Iron Dust | 4 - 20 |
| Smoke from Synthetic Materials | 1 - 50 |
| Lead Dust | 2 |
| Face Powder | 0.1 - 30 |
| Talcum Dust | 0.5 - 50 |
| Asbestos | 0.7 - 90 |
| Calcium Zinc Dust | 0.7 - 20 |
| Paint Pigments | 0.1 - 5 |
| Auto and Car Emission | 1 - 150 |
| Metallurgical Dust | 0.1 - 1000 |
| Metallurgical Fumes | 0.1 - 1000 |
| Clay | 0.1 - 50 |
| Humidifier | 0.9 - 3 |

| Particle | Particle Size (microns) |
|-----------------------------------|----------------------------|
| Copier Toner | 0.5 - 15 |
| Liquid Droplets | 0.5 - 5 |
| Insecticide Dusts | 0.5 - 10 |
| Anthrax | 1 - 5 |
| Yeast Cells | 1 - 50 |
| Carbon Black Dust | 0.2 - 10 |
| Atmospheric Dust | 0.001 - 40 |
| Smoldering or Flaming Cooking Oil | 0.03 - 0.9 |
| Corn Starch | 0.1 - 0.8 |
| Sea Salt | 0.035 - 0.5 |
| Bacteria | 0.3 - 60 |
| Bromine | 0.1 - 0.7 |
| Lead | 0.1 - 0.7 |
| Radioactive Fallout | 0.1 - 10 |
| Rosin Smoke | 0.01 - 1 |
| Combustion | 0.01 - 0.1 |
| Smoke from Natural Materials | 0.01 - 0.1 |
| Burning Wood | 0.2 - 3 |
| Coal Flue Gas | 0.08 - 0.2 |
| Oil Smoke | 0.03 - 1 |
| Tobacco Smoke | 0.01 - 4 |
| Viruses | 0.005 - 0.3 |
| Typical Atmospheric Dust | 0.001 to 30 |
| Sugars | 0.0008 - 0.005 |
| Pesticides & Herbicides | 0.001 |
| Carbon Dioxide | 0.00065 |
| Oxygen | 0.0005 |

BIBLIOGRAPHY:

Albayrak A., W. J., Petrenko M., Lynnes C., Levyb R. C. . (2013). Global bias adjustment for MODIS aerosol optical thickness using neural network. *Journal of Applied Remote Sensing*, 7(1), 073514-073514.

Bilal, M., Nichol, J. E., Bleiweiss, M. P., & Dubois, D. (2013). A Simplified high resolution MODIS Aerosol Retrieval Algorithm (SARA) for use over mixed surfaces. *Remote Sensing of Environment*, 136(0), 135-145. doi: <http://dx.doi.org/10.1016/j.rse.2013.04.014>

Bucholtz, A. (1995). Rayleigh-scattering calculations for the terrestrial atmosphere. *Applied Optics*, 34(15), 2765-2773.

Cassell, B. (2014). Utility plans partial conversion to gas, new air controls at remaining coal unit, from http://generationhub.com/pages/article_print.php?aid=2014/02/07/sierra-club-wants-coal-gone-at-harding-street-plan

Chudnovsky, A., Tang, C., Lyapustin, A., Wang, Y., Schwartz, J., & Koutrakis, P. (2013). A critical assessment of high-resolution aerosol optical depth retrievals for fine particulate matter predictions. *Atmospheric Chemistry and Physics*, 13(21), 10907-10917.

Dominici, F., Peng, R. D., Bell, M. L., & et al. (2006). Fine particulate air pollution and hospital admission for cardiovascular and respiratory diseases. *JAMA*, 295(10), 1127-1134. doi: 10.1001/jama.295.10.1127

Engel-Cox, J. A., Holloman, C. H., Coutant, B. W., & Hoff, R. M. (2004). Qualitative and quantitative evaluation of MODIS satellite sensor data for regional and urban scale air quality. *Atmospheric Environment*, 38(16), 2495-2509.

EPA_Team. (2013). Particulate Matter (PM), from <http://www.epa.gov/air/particlepollution/>

Hauser, A., Oesch, D., & Wunderle, S. (2004). Retrieval of aerosol optical depth (AOD) using NOAA AVHRR data in an alpine environment. Paper presented at the Remote Sensing.

Hoff, R. M., & Christopher, S. A. (2009). Remote sensing of particulate pollution from space: have we reached the promised land? *Journal of the Air & Waste Management Association*, 59(6), 645-675.

Hsu, N. C., Tsay, S.-C., King, M. D., & Herman, J. R. (2006). Deep blue retrievals of Asian aerosol properties during ACE-Asia. *Geoscience and Remote Sensing, IEEE Transactions on*, 44(11), 3180-3195.

Hu, Z. (2009). Quantitative Evaluation of Satellite Aerosol Data for Mapping Fine Particulate Air Pollution in the Conterminous United States. Paper presented at the The 24th International Cartography Conference, Santiago, Chile.

Jo Alfano, M., Biehl, L., Ensign, T., Landenberger, R., O'Neill, M., & Somers-Austin, C. (2013). Exploring Aerosol Optical Thickness Using MODIS Satellite Imagery in NEO, from <http://serc.carleton.edu/usingdata/datasheets/aerosolopticalthick.html>

Kaufman, Y. J., & Tanré, D. (1998). Algorithm for remote sensing of tropospheric aerosol from MODIS. NASA MODIS Algorithm Theoretical Basis Document, Goddard Space Flight Center, 85.

Koelemeijer, R., De Haan, J., & Stammes, P. (2003). A database of spectral surface reflectivity in the range 335–772 nm derived from 5.5 years of GOME observations. *Journal of Geophysical Research: Atmospheres* (1984–2012), 108(D2).

Kwon Ho, L., Young Joon, K., von Hoyningen-Huene, W., & Burrow, J. P. (2006). Influence of land surface effects on MODIS aerosol retrieval using the BAER method over Korea. *International Journal of Remote Sensing*, 27(14), 2813-2830.

Li, C., Lau, A.-H., Mao, J., & Chu, D. A. (2005). Retrieval, validation, and application of the 1-km aerosol optical depth from MODIS measurements over Hong Kong. *Geoscience and Remote Sensing, IEEE Transactions on*, 43(11), 2650-2658.

Li, Y., Xue, Y., He, X., & Guang, J. (2012). High-resolution aerosol remote sensing retrieval over urban areas by synergetic use of HJ-1 CCD and MODIS data. *Atmospheric Environment*, 46(0), 173-180. doi: <http://dx.doi.org/10.1016/j.atmosenv.2011.10.002>

Liu, Y., Hu, M., Pan, X., Shi, J., Chen, F., Koutrakis, P., . . . Wang, Z. (2011). Application Of Satellite Aerosol Remote Sensing Technology To Estimate The Acute Health Impacts Of Airborne Particles. *Science*, 1(2), 3.

Mei, L., Xue, Y., Guang, J., Li, Y., Wan, Y., Bai, L., & Ai, J. (2009). Aerosol optical depth retrieval over land using MODIS data and its application in monitoring air quality. Paper presented at the Geoscience and Remote Sensing Symposium, 2009 IEEE International, IGARSS 2009.

n.p. (Retrieved August 12, 2014). Sizes of airborne particle from http://www.engineeringtoolbox.com/particle-sizes-d_934.html

NASA, M. (Retrieved November 7th, 2014). MODIS Specifications from <http://modis.gsfc.nasa.gov/about/specifications.php>

Qu, J. J., Gao, W., Kafatos, M., Murphy, R. E., & Salomonson, V. V. (2006). *Earth Science Satellite Remote Sensing Vol. 1: Science and Instruments*. Berlin, Heidelberg: Co-published by Tsinghua University Press, Beijing and Springer-Verlag GmbH Berlin Heidelberg.

Remer, L. A., Kaufman, Y., Tanré, D., Mattoo, S., Chu, D., Martins, J. V., . . . Kleidman, R. (2005). The MODIS aerosol algorithm, products, and validation. *Journal of the atmospheric sciences*, 62(4).

Remer, L. A., Tanre, D., Kaufman, Y. J., Levy, R., & Mattoo, S. (2006). Algorithm for remote sensing of tropospheric aerosol from MODIS: Collection 005. National Aeronautics and Space Administration.

Seaton, A., Godden, D., MacNee, W., & Donaldson, K. (1995). Particulate air pollution and acute health effects. *The Lancet*, 345(8943), 176-178. doi: [http://dx.doi.org/10.1016/S0140-6736\(95\)90173-6](http://dx.doi.org/10.1016/S0140-6736(95)90173-6)

Toller, G. N., Isaacman, A., Leader, M. T., & Salomonson, V. (2003). MODIS Level 1B Product User's Guide. Signature.

Vermote, E. F., El Saleous, N. Z., & Justice, C. O. (2002). Atmospheric correction of MODIS data in the visible to middle infrared: first results. *Remote Sensing of Environment*, 83(1–2), 97-111. doi: [http://dx.doi.org/10.1016/S0034-4257\(02\)00089-5](http://dx.doi.org/10.1016/S0034-4257(02)00089-5)

von Hoyningen-Huene, W., Freitag, M., & Burrows, J. (2003). Retrieval of aerosol optical thickness over land surfaces from top-of-atmosphere radiance. *Journal of Geophysical Research: Atmospheres* (1984–2012), 108(D9).

wikipedia. (Retrieved November 1st 2014). Indiana from <http://en.wikipedia.org/wiki/Indiana#Geography>

Wong, M. (2009). Retrieval of aerosol optical thickness at 500m resolution using MODIS images: a study in Hong Kong and the Pearl River Delta region. The Hong Kong Polytechnic University.

Wong, M., Nichol, J., Lee, K. H., & Li, Z. (2009). High resolution aerosol optical thickness retrieval over the Pearl River Delta region with improved aerosol modelling. *Science in China Series D: Earth Sciences*, 52(10), 1641-1649.

Wong, M. S., Nichol, J. E., & Lee, K. H. (2011). An operational MODIS aerosol retrieval algorithm at high spatial resolution, and its application over a complex urban region. *Atmospheric Research*, 99(3–4), 579-589. doi: <http://dx.doi.org/10.1016/j.atmosres.2010.12.015>

Xiong, X., Isaacman, A., & Barnes, W. (2006). MODIS level-1B products Earth science satellite remote sensing (pp. 33-49): Springer.

Zhao, L., Wu, S., Veeramacheneni, R., Song, C. X., & Biehl, L. (2009). Delivering real-time satellite data to a broader audience. Paper presented at the Proceedings of the 5th Grid Computing Environments Workshop.

CURRICULUM VITAE
FAHED ALHAJ MOHAMAD

Education and training:

Master of Science: Geographic Information Science (Fulbright sponsorship), 05/2015

Indiana University - Indianapolis, IN

Bachelor of Art: Geography, Specializing in Cartography and GIS, 07/2008

Damascus University - Damascus, Syria

Professional experience:

GIS Analyst Intern: May 2013 to August 2013, SmartZip Analytics Inc., Pleasanton, CA.

GIS Analyst: February 2010 to July 2012, IbdAA for Intelligent Solutions, Damascus, Syria.

Honors and awards:

Fulbright scholarship grantee: 2012 – 2014.